Laser Cavity Density Changes with Kinetics of Energy Release

OSCAR BIBLARZ* AND ALLEN E. FUHS†
Naval Postgraduate School, Monterey, Calif.

Inherent in any lasing process involving three or more energy levels is the release of heat. The heat is the inefficiency implied in the definition of laser quantum efficiency. In supersonic flow the heat release causes compression waves and a wake, thereby perturbing the gas density. Gas density variations within the laser cavity degrade the beam quality. A comprehensive analysis was made using an extension of the Tsien-Beilock linearized solution for heat addition. A computer program has been developed which incorporates multiple wall reflections, arbitrary beam cross section, and finite kinetics for the transition from the lower laser level to the ground state. Several examples are discussed. Uniform energy release in a rectangular cavity without reflections and without lag for heat addition, with lag and no reflections, and with both lag and reflections has been calculated. A rectangular cavity with a gaussian energy release distribution without lag and with reflections and with both lag and wall reflections has been analyzed. This case is representative of a master-oscillator-power-amplifier arrangement. Finally an energy release distribution in the shape of a crescent was calculated. The crescent was located with convex side upstream and with the peak upstream of the cavity axis. Fractional density perturbation greater than 1% was found for typical conditions in a gas dynamic laser. Larger perturbations would be expected in lasers with a larger output.

Nomenclature

a	= speed of sound
E_v	= vibrational energy of lower laser level
E_v^*	= equilibrium value of E_v
H	= total heat release due to lasing action
$h(x, y, z)$	= heat addition function, energy/(time) (volume)
I	= total laser radiation output, w
$I(x)$	= unit function; zero for $x < 0$ and unity for $x \geqq 0$
i	= laser energy per unit area at aperture, w/cm^2
l	= length of laser beam within cavity
L	= length of wake within the heat addition zone (laser cavity) upstream of observation point
M	= Mach number
p	= static pressure
q	= strength of line heat source, energy/(time) (length)
S	= distance along a characteristic
S_L	= length of left running characteristic immersed in heat addition zone (laser cavity)
S_R	= length of right running characteristic immersed in heat addition zone (laser cavity)
t	= time
U	= velocity of gas in laser cavity
v'	= velocity perturbation in y-direction
u'	= velocity perturbation in x-direction
x	= coordinate in flow direction
x_d	= coordinate of downstream edge of laser beam
x_u	= coordinate of upstream edge of laser beam
y	= coordinate normal to flow direction
z	= coordinate along beam path
w	= width of cavity; see Fig. 14
β^2	= $(1-M^2)$ for subsonic flow; M^2-1 for supersonic flow
γ	= ratio of heat capacities
δ	= delta function
η	= laser quantum efficiency
μ	= Mach angle defined by arc sin $(1/M)$
ρ	= density, mass/volume
τ	= vibrational relaxation time

Presented as Paper 73-141 at the AIAA 11th Aerospace Sciences Meeting, Washington, D.C., January 10–12, 1973; submitted January 31, 1973; revision received November 6, 1973. This work reflects research supported by the Air Force Weapons Laboratory, Kirtland Air Force Base, under Project Order 72PO73101.

Index categories: Lasers; Supersonic and Hypersonic Flow.

* Associate Professor of Aeronautics. Member AIAA.

† Professor of Aeronautics. Associate Fellow AIAA.

Introduction

QUANTUM efficiency of a laser is defined as the energy difference between the upper and lower laser levels divided by the energy difference between upper level and the ground state. The energy difference between lower laser level and ground state is a loss and appears as heat. It is obvious that it is not possible to have lasing action without this loss—the heat addition is inherent for a three-level lasing process.

In the case of the CO_2 laser operating at 10.6μ, the quantum efficiency is approximately 40%. This means 60% of the upper laser level appears as heat in the gas. The heat will not appear simultaneously with the laser radiation but will lag. The kinetics of the lag are important.

Heat addition in a supersonic stream causes compression waves which radiate from the heat release region. The waves reflect from the cavity walls. Downstream of the heat release region is a wake. Whereas the compression waves increase gas density, the wake decreases gas density. The wake has gas at a higher static temperature.

Although supersonic flow will be featured, the theory developed herein also is applicable with minor modifications to subsonic flow. Heat addition in a subsonic flow causes a wake in much the same manner as for supersonic flow. However, there are no compression waves; the influence of the heat addition extends throughout the flow region. Thus the theory is applicable to CW flowing lasers, either subsonic or supersonic.

Density gradients within the laser cavity degrade beam quality. From the geometric optics point of view, light is refracted within the laser cavity causing beam spread in a manner analogous to thermal blooming. From the point of view of diffraction theory, the density variations cause a nonuniform phase distribution over the laser exit aperture. Beam quality calculations are not included in this paper but will be the topic of a subsequent one. The results contained herein are directly applicable to beam quality calculations.

Considerable effort has been devoted by engineers and scientists working with both pulsed and CW lasers to measure, analyze, and correct density variations.[1-11] For the case of pulsed lasers,[5,6] the density change due to energy release has been investigated. For the case of steady flow lasers, e.g., gas dynamic lasers, the influence of wakes from struts or nozzles, boundary layers, and wall irregularities on density perturbation have been investigated. As discussed above, yet another mechanism exists

to cause density gradients, and it appears that this mechanism has been overlooked.

Heat Addition

Tsien and Beilock[12] obtained solutions for the linearized equations of motion with heat addition for both subsonic and supersonic flow. The solutions are for a line heat source in a uniform, two-dimensional planar flow. Although this paper treats the supersonic case, the subsonic solutions are stated here to emphasize the fact that the method is generally applicable.

If the variation of the radiation intensity in the beam direction (z-direction) is small, then the two-dimensional planar solutions of Tsien and Beilock correctly describe density perturbations due to lasing. However, if there is significant change in the z-direction, then three-dimensional solutions would be needed. There are two extreme cases that one can consider with regard to intensity variation along the beam. A single-pass amplifier would have large changes in intensity. A high-Q oscillator, e.g., an optical cavity with low-output coupling, would be nearly two dimensional. In any case in between these extremes, the distribution of phase at the exit aperture represents an integration along the rays, thereby averaging the influence of nonuniform intensity. Experiments[13] have been conducted to verify the validity of the theory developed in this paper. The excellent agreement between theory and experiments tends to confirm the adequacy of the theory at least for unstable-oscillator optical configurations.

Subsonic Flow with Heat Addition

The perturbations to the flow are given by

$$u' = (\gamma-1)qx/2\pi\gamma p\beta(x^2+\beta^2y^2) \tag{1}$$

$$v' = (\gamma-1)\beta qy/2\pi\gamma p(x^2+\beta^2y^2) \tag{2}$$

$$p' = (\gamma-1)Mqx/2\pi a\beta(x^2+\beta^2y^2) \tag{3}$$

$$\rho' = -\frac{(\gamma-1)Mq}{2\pi a^3\beta}\left[\frac{x}{x^2+\beta^2y^2}\right] - \frac{(\gamma-1)q}{Ma^3}\delta(y)I(x) \tag{4}$$

The symbols are defined in the Nomenclature. A prime indicates a perturbation quantity; the second term in Eq. (4) is the wake of the heat source q.

Supersonic Flow with Heat Addition

Equations similar to Eqs. (1–4) are given in the paper by Tsien and Beilock.[12] The density perturbation has been modified by Fuhs[14,15] into an integral form

$$\frac{\Delta\rho(x,y)}{\rho} = \frac{(\gamma-1)/M}{2a^3\beta\rho}\int_0^S h(x',y')\sin\mu\,dS - \frac{(\gamma-1)}{a^2U\rho}\int_{x'}\int_{y'} h(x',y')\delta(y-y')I(x-x')\,dx'\,dy' \tag{5}$$

The units for h are energy/(time)(volume). The volume can be interpreted as an area times the span of the heat addition zone across the planar flow. The wake is represented by the second integral on the right-hand side of Eq. (5).

An approximate approach can be used when there is significant variation of beam intensity in the z-direction. The two-dimensional heat addition function can be obtained from the three-dimensional $h(x, y, z)$ by an average,

$$h(x,y) = \frac{1}{\Delta z}\int_{z_i}^{z_{i+1}} h(x,y,z)\,dz \tag{6}$$

where $\Delta z = z_{i+1} - z_i$. The beam is divided into segments Δz in length, and Eq. (5) is solved for each segment. Beam quality calculations would use the appropriate $\Delta\rho/\rho$ calculated for each segment.

Application to Lasers

To clearly demonstrate the application of Eq. (5) to the flow in laser cavities, the case of uniform heat release will be discussed. Furthermore, the influence of reflection of waves at the wall and the lag of heat release will be ignored at first. Following the simplified problem, the general case of nonuniform heat release including reflections and lag will be formulated.

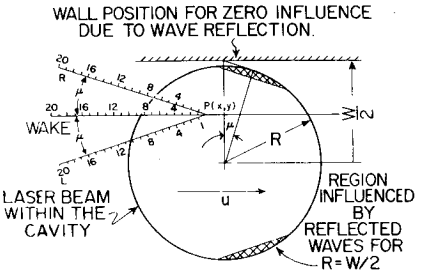

Fig. 1 Illustration of computational procedure (reproduced from Ref. 14).

Calculation Procedure for Uniform Energy Release[15]

When h equals a constant in Eq. (5) the integrals can be readily evaluated. For a uniform profile entering the laser cavity, $\sin\mu$ is a constant. Consequently $\Delta\rho/\rho$ depends only on geometry, and a semigraphical calculation procedure is appropriate. The procedure is illustrated in Fig. 1. At point P, the compression is due to the heat sources along the right and left running characteristics and to the wake upstream of P. In fact, it is only the lengths of the wake and characteristics which determine $\Delta\rho/\rho$ once the constants have been evaluated. In Fig. 1, the length of the right running characteristic R immersed in the heat addition zone (laser cavity) is 7.0 and that of the left running characteristic is 10.0. The wake is 8.4 units of length. For uniform heat release

$$\Delta\rho/\rho = C_1(S_R + S_L) + C_2 L$$

For typical conditions[15] the value of C_1 is $+0.023$/ft and C_2 is -0.052/ft. For nonuniform heat release the calculation procedure is similar except that each element of characteristic length is weighed by $\sin\mu h(x', y')$ and each element of wake length is weighted by $h(x', y')$.

Calculation Procedure for Nonuniform Energy Release

Without wall reflections and without kinetic lag, Eq. (5) is evaluated using the geometry of Fig. 1. With wall reflections, the concept of an image heat addition zone can be introduced as shown in Fig. 2. At the wall v' must be zero. Use of an image heat addition zone satisfies the wall boundary condition. The density perturbation at point P in Fig. 2 is due, in part, to a right

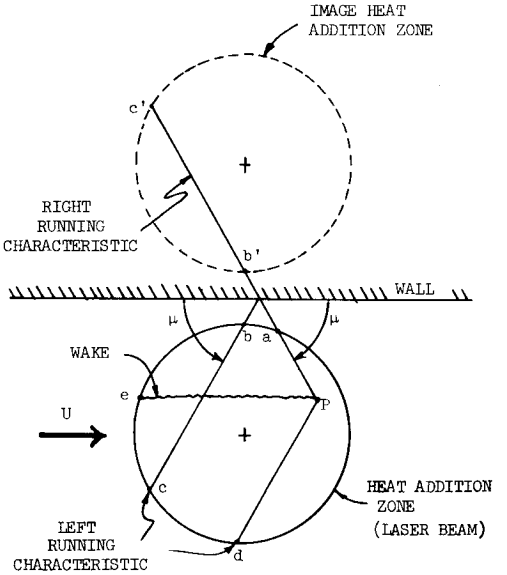

Fig. 2 Image for wall reflection.

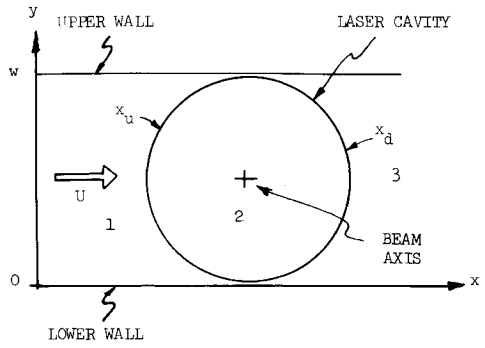

Fig. 3 Coordinate system for describing vibrational relaxation.

running compression wave for which the integral of Eq. (5) is non-zero from P to a and from b' to c'.

The left running characteristic along Pd contributes to $\Delta\rho/\rho$, and the wake from P to e has an influence. The effect of a right running characteristic from b' to c' is identical to the influence of the left running characteristic along b to c. To incorporate wall reflections, the characteristics are plotted upstream from point P and reflected at walls. Any part of the characteristic traversing the heat addition zone contributes to the integral in Eq. (5).

To develop an equation incorporating the time lag between lasing and heat release, it is necessary to examine the kinetics of vibrational-translational relaxation. For the geometry of Fig. 3 there are three distinct regions as follows: Region 1, $0 < x < x_u$; Region 2, $x_u < x < x_d$; and Region 3, $x_d < x < \infty$. Since great effort is devoted to achieving uniform flow across the $x = 0$ plane, $\Delta\rho/\rho$ in Region 1 can be precisely calculated by Rayleigh flow. The vibrational relaxation rates must be known to find $h(x)$; there is no y- or z-dependence in Region 1.

For the discussion of Regions 2 and 3, the notation of Hoffman and Vlases[16] will be used. In Region 2, the lasing process dominates the competitive collisional depopulation process characterized by τ_8. Consequently, the heat release is due to the collisional process subsequent to lasing denoted as τ_1 by Hoffman and Vlases. A single relaxation time can be used in Region 2; the appropriate[17-20] equation for the heat addition function is

$$h(x,y) = C\int_{x_u}^{x} i(x',y)\exp\left[-(x-x')/U\tau\right]dx' \qquad (7)$$

The function $h(x, y)$ is the heat added at x and y; $h(x, y)$ is not the cumulative heat added in a streamtube upstream of x. A derivation of $h(x, y)$ is shown in the Appendix. The function $i(x, y)$ is the power density in w/cm^2 at the laser exit aperture. The constant C, which has units of cm^{-2}, can be evaluated from an energy balance. Strictly speaking, Eq. (7) is valid only in Region 2. The selection of the proper value for τ is outlined in Biblarz and Fuhs[21] [see Eqs. (21), and (30–33) of Ref. 21].

Since the flow is supersonic, Regions 1 and 2 are not affected by Region 3. To calculate $\Delta\rho/\rho$ in Regions 1 and 2, one can ignore Region 3. However, for multipass lasers, it is necessary to determine $\Delta\rho/\rho$ in Region 3. Here, in contrast to Region 1, Rayleigh flow solutions do not apply. Consider a streamtube passing through the beam axis where the populations of CO_2 (001) and N_2 (1) are almost depleted. Now consider a streamtube passing through the edge of the beam for which there has been little power extraction and for which the populations of CO_2 (001) and N_2 (1) remain large. It should be apparent from this discussion that the populations differ from streamtube to streamtube and that the use of Eq. (5) is needed for each case. In principle, a relaxation model involving two relaxation times (two-τ model) is required for Region 3. Equation (21) of Ref. 21 gives the formula for $h(x, y)$ in Region 3.

The spatial distribution of heat release in Region 3 causes $\Delta\rho/\rho$ changes which oppose those resulting from Region 2. One set of calculations were made for Region 3 using a two-τ model. These calculations were compared to the results obtained by applying Eq. (7) to Region 3. Note that the $h(x, y)$ predicted by Eq. (7) is not zero for $x > x_d$. The comparison showed that the error was small if Eq. (7) is used for the heat addition function in Region 3. Experiments[13] undertaken so far tend to confirm the analysis.

The use of Eq. (7) in Region 3 has the distinct advantage that it is not necessary to know the detailed kinetics within each streamtube to apply the theory. It is, of course, necessary to know $i(x, y)$ and $h(x, y)$. All calculations in this paper were made using Eq. (7) for $h(x, y)$.

By integrating $h(x, y)$ one obtains the total heat release

$$H = Cl\int_0^w\int_{x_u}^{\infty}\int_{x_u}^{x} i(x',y)\exp\left[-(x-x')/U\tau\right]dx'\,dx\,dy \qquad (8)$$

where l is the cavity length in the z-direction. Likewise an integration of i yields the total radiation output

$$I = \int_0^w\int_{x_u}^{x_d} i(x',y)\,dx'\,dy \qquad (9)$$

The laser quantum efficiency η can be used to relate H and I, thus,

$$(H/I) = (1-\eta)/\eta \qquad (10)$$

It is apparent that Eqs. (8–10) can be combined and solved for C. Knowing C one can combine Eqs. (5) and (7) to obtain an equation incorporating the lag due to vibrational relaxation.

Computer Program

This program was written to calculate density changes in supersonic flow. Equation (5) describes the separate contributions due to heat release. The program calculates the two-dimensional field at any cross section of the laser beam where the energy release distribution is known. Finite kinetics are incorporated as described by Eqs. (5), and (7–10). Multiple wall reflections of the characteristic lines are included in the program.

The main feature of the program is that the discretized two-dimensional field consists of rectangular cells whose size is determined by the Mach angle. The ratio of cell height Δy to cell length Δx is equal to tan μ. The program sets up the characteristic lines belonging to each individual cell and adds up the contributions to the density change from the characteristics and from the wake at each cell. The calculations along the characteristics are facilitated by the choice of cell size and reflections take place at the cells in the upper and lower walls. Multiple reflections or no reflections can be handled. The geometry of the laser beam and of the cavity are all that is necessary for the computer to trace the heat release moving along the characteristics.

In its present form, the program treats only uniform velocity profiles across the beam with no shocks present. Also, the intensity data is not coupled to the density inhomogeneity, i.e., they are independently treated. The intensity would come typically from experimental observation.

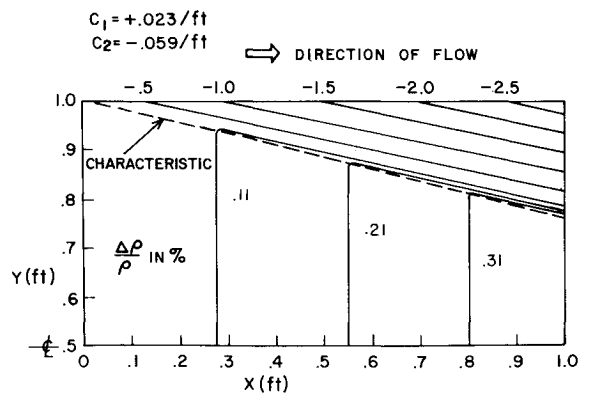

Fig. 4 $\Delta\rho/\rho$ contours in a square cavity without kinetics or reflections.

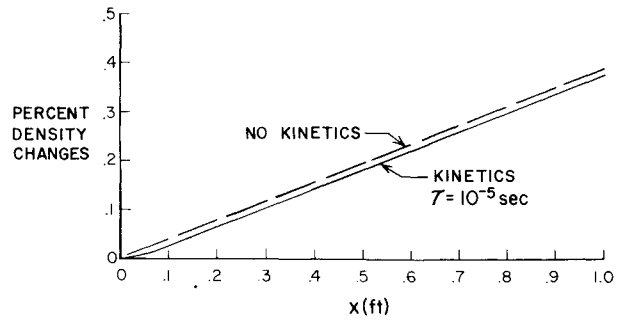

Fig. 5 Density distribution in the square cavity midplane with and without kinetics.

Results of Calculations

A supersonic flow at Mach 4 was used for the calculations that follow where various energy distributions are considered.

Rectangular Cavity with Uniform Release

In order to check the computer program, the rectangular cavity with uniform release and no reflections or lag was calculated. The results, which agreed with Fig. 3 of Fuhs,[15] are shown in Fig. 4. The density increases moving along the cavity midplane. Calculations were repeated including kinetics with $\tau = 10^{-5}$ sec. The density variation along the cavity midplane is plotted in Fig. 5. With kinetics, the density variation starts from zero at the cavity leading edge and smoothly changes to a positive slope. The curve with kinetics is displaced downstream. For the case illustrated, U was approximately 4000 fps and the cavity width was 1 ft. The value of $U\tau/L$ is 0.04 which is approximately the distance the curve is displaced downstream. Figure 5 is also applicable to the square cavity with wall reflections.

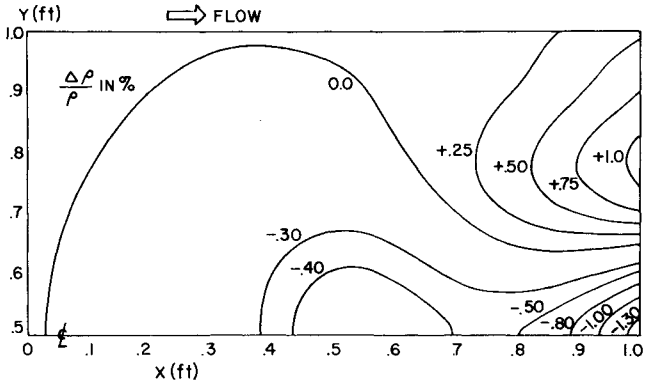

Fig. 6 Isodensity contours for the gaussian distribution, $\tau = 10^{-5}$ sec.

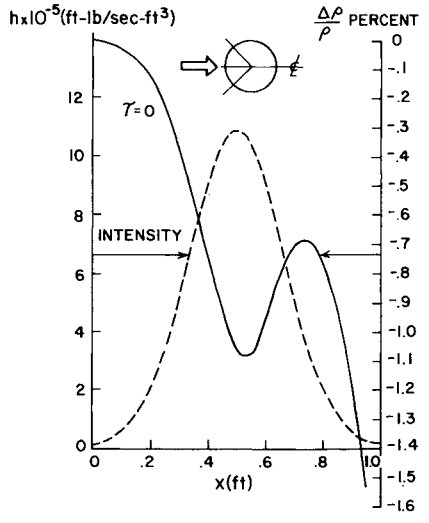

Fig. 7 Centerline density distribution for the gaussian without kinetics.

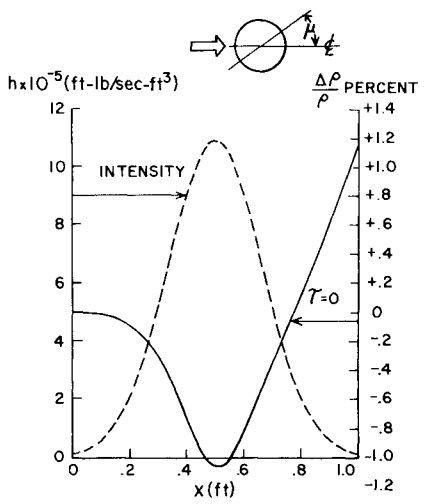

Fig. 8 Left running characteristic through the midpoint without kinetics.

Gaussian Energy Release Distribution

When a laser cavity serves as an amplifier, the laser radiation intensity distribution frequently has a gaussian profile. For this reason calculations were performed using the gaussian distribution. The isodensity contours are shown in Fig. 6. Note that the wake of the central gaussian peak is evident downstream. For Fig. 6, τ is assumed to be 10^{-5} sec.

Since the ray equation of geometric optics[22] contains the gradient of the index of refraction, curves of constant density changes have been plotted. By the Gladstone-Dale constant,[23] density and index of refraction are related. Figure 7 shows $\Delta\rho/\rho$ for the case of zero τ. The density gradients are of a shape to cause beam spread. While Fig. 7 shows density changes along the laser midplane, Fig. 8 shows the density variation along the left-running characteristic that passes through the axis of the gaussian distribution where it is seen that the density variation is more symmetrical. Figure 9 shows that the midplane density changes with increasing kinetics and that the minimum in the curve disappears with increasing τ. Thus, the beam sees only an increasing density upstream.

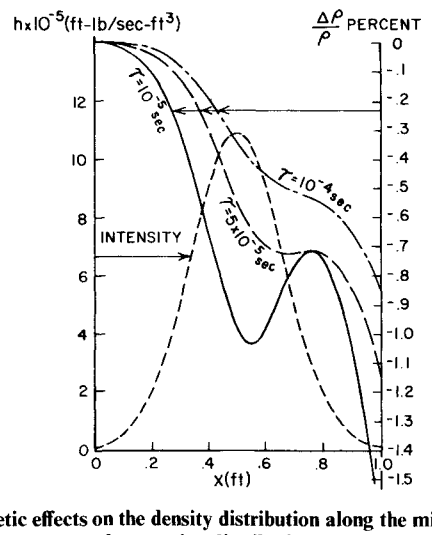

Fig. 9 Kinetic effects on the density distribution along the midplane for the gaussian distribution.

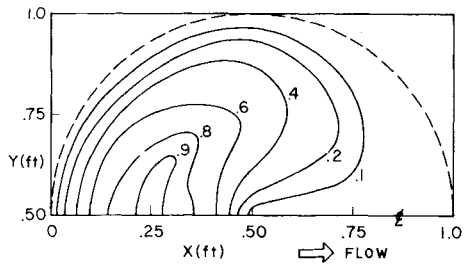

Fig. 10 Crescent-shaped intensity distribution.

In these calculations an average output of 9 kjoules per pound has been assumed with a flow rate of 40 lbm/sec. The gaussian intensity at the edges of the beam is less than 1% of that at the midpoint.

Crescent-Shape Energy Release Distribution

The crescent-shape distribution is another practical example of nonhomogeneous energy release within the laser beam. The crescent shapes were generated with an arbitrary set of functions which locate the crescent with convex side upstream and with the peak upstream of the cavity axis. The energy distribution used is shown in Fig. 10. The peak power is the same as that in the gaussian distribution. Figure 11 shows the isodensity contours.

Density changes along the laser midplane are shown in Fig. 12, including wall reflections but without kinetics. Figure 13 shows what happens to the midplane density changes with increasing kinetics. While the minimum does not disappear here, it flattens out considerably and moves downstream. Because of this motion downstream, the most intense part of the beam sees a change upstream steeper than downstream.

Comments on Results

The main purpose of this paper has been to describe the method for calculating $\Delta\rho/\rho$ in CW flowing (supersonic) lasers. The preceding section has illustrated the variations in $\Delta\rho/\rho$ for several realistic laser intensity profiles. In this section some suggestions are made for utilization of the $\Delta\rho/\rho$ contour maps.

Geometric Optics Approximation

Clark[24] discusses briefly thermal blooming internal to the laser cavity. In a series of papers, scientists at Naval Research Laboratory[25-28] discuss thermal blooming using the ray equation. Since $\Delta\rho/\rho$ is known from the calculations of this paper, an estimate can be made of beam spreading.

Clark[24] also indicates that the beam internal to the laser cavity experiences deflections analogous to the beam-in-the-wind problem. This is a nonlinear problem in which the solution of Eq. (5) is coupled to the heat release within the cavity.

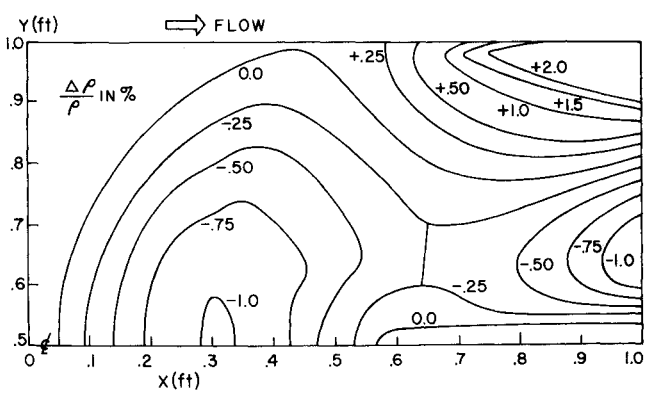

Fig. 11 Isodensity contours for the crescent-shaped intensity distribution, $\tau = 10^{-5}$ sec.

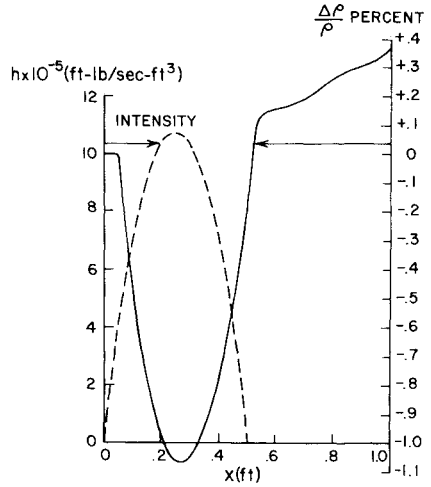

Fig. 12 Midplane density distribution for the crescent, without kinetics.

Diffraction Theory

An alternate approach can be taken for estimating the influence of $\Delta\rho/\rho$. The laser cavity with uniform density establishes certain phase relations at laser exit aperture. As a result of the density variations the phase distribution at the exit aperture is altered. Kirchhoff's integral[29] could be applied for determining external beam intensity distribution.

A particularly simple model would be to assume a plane wave at the end of the laser beam opposite the exit. The phase variations caused by $\Delta\rho/\rho$ could be determined at the exit and then Kirchhoff's integral could be evaluated.

Repetition of Wave Pattern

Figure 14a illustrates the repetition of a wave pattern in a wind tunnel. The flow disturbances downstream are identical (neglecting viscous effects) to those that would exist if the body were actually repeated. This fact suggests an experiment to verify the theory and calculations reported herein.

According to Fig. 14b point P' in window B has the same $\Delta\rho/\rho$ as point P in window A, once a correction has been made for the influence of the wake. The upstream region at window A could be a laser cavity. The downstream region at window B could be a diagnostic region. Holographic interferometry could yield the $\Delta\rho/\rho$ caused by lasing in the region of window A.

An experiment similar to the one suggested in the preceding paragraphs has been performed and results are in good agreement

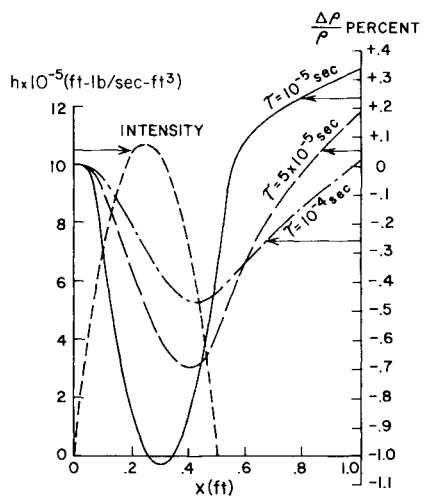

Fig. 13 Kinetic effects on the midplane density distribution for the crescent.

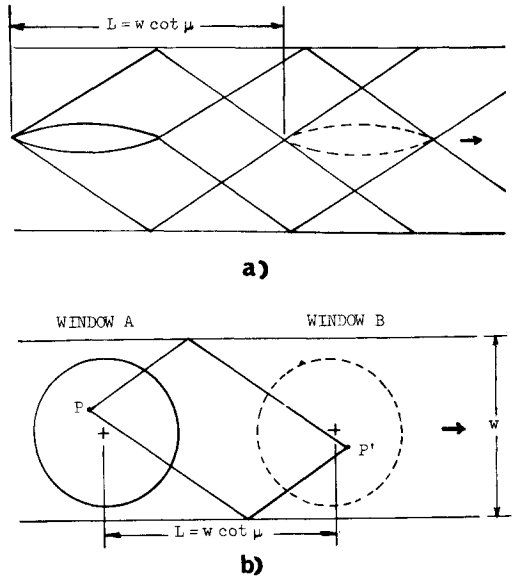

Fig. 14 Images repeated downstream. a) Repetition of wave pattern in a wind tunnel. b) Repetition of wave pattern in a laser.

with the theoretical calculations.[13] Success of the experiment suggests that in the case of a GDL cavity, the boundary layers do not strongly affect the reflections which were assumed to be specular.

Nonuniform Flow Profiles

The profiles in Mach number, entropy, and velocity may not be uniform at the entrance to the laser cavity. This paper assumes a uniform input of flow variables. Using reflection coefficients as discussed by Refs. 30–33, the theory can be modified to include nonuniform profiles.

Conclusions

Calculations have been made for density changes in a supersonic flow due to a heat addition intrinsic to the lasing process. With reasonable although arbitrary energy distributions changes in $\Delta\rho/\rho$ of 1% have been found. The linearized theory for density changes due to heat addition used here appears to be an accurate description of the problem. The computer program results show that the inclusion of wall reflections and of kinetics cause noticeable changes in the results. Hence, for any calculations to be useful in the laboratory, all these factors must be included. The utilization of these results may lead to improved design in laser cavities.

Appendix

This Appendix derives Eq. (7). If one considers a simplified model[21] of the N_2-CO_2 system where the depopulation of the lower laser level is the dominant V-T process, then

$$(dE_v/dt) = \frac{1}{\tau}(E_v^* - E_v) \tag{A1}$$

Here, E_v is the energy of the lower laser level with respect to ground and E_v^* is the equilibrium value corresponding to the temperature at that level. τ is the appropriate relaxation time. Because of the lasing process, it is assumed that $E_v \gg E_v^*$. Since the flow is essentially one dimensional, we can write

$$(dE_v/dt) = U(dE_v/dx) = -(E_v/\tau) \tag{A2}$$

or

$$\int \frac{dE_v}{E_v} = -\int_{x'}^{x} \frac{dx}{U\tau}$$

Now, assuming that both U and τ are constant, integration yields

$$E_v(x, y) = E_v(x', y)\exp[-(x-x')/U\tau] \tag{A3}$$

The above result indicates that lasing at x' may release some of the vibrational energy as heat at a station x downstream. The magnitude of this delayed heat release, of course, depends strongly on the term $U\tau$ in the exponent.

Since we assume that the population of the lower laser level is due entirely to lasing, the energy E_v is proportional to the intensity i of the laser beam at each cross section along the beam path. The total heat release at x will depend on the residuals of the upstream heat release locations due to the kinetic lag, i.e.,

$$h(x, y) = \int_{x_u}^{x} E_v(x', y)\exp[-(x-x')/U\tau]\,dx'$$

$$= C\int_{x_u}^{x} i(x', y)\exp[-(x-x')/U\tau]\,dx'$$

Evaluation of the constant C has been outlined in the discussion of Eqs. (9) and (10).

References

[1] Emmett, J. L., "Frontiers of Laser Development," *Physics Today*, Vol. 24, No. 3, March 1971, pp. 24–31.

[2] Anderson, J. D., Jr. and Harris, E. L., "Modern Advances in the Physics of Gasdynamic Lasers," AIAA Paper 72-143, San Diego, Calif., 1972.

[3] Hoffman, A. and Jones, T., "Geometric Methods for Improving the Optical Quality of Gas Dynamic Laser," AIAA Paper 72-217, San Diego, Calif., 1972.

[4] Simons, G. A., "The Effect of Boundary Layers on GDL Medium Homogeneity," AIAA Paper 72-709, Boston, Mass., 1972.

[5] O'Neill, R. W., Carbone, R. J., Granek, H., and Kleiman, H., "TEA Laser Medium Diagnostics," *Applied Physics Letters*, Vol. 20, No. 11, June 1972, pp. 461–463.

[6] Longaker, P. R. and Litvak, M. M., "Perturbation of the Refractive Index of Absorbing Media by a Pulsed Laser Beam," *Journal of Applied Physics*, Vol. 40, No. 10, Sept. 1969, pp. 4033–4041.

[7] Otis, G. and Tremblay, R., "Lensing Effects in Helical TEA-CO_2 Laser," *Journal of the Optical Society of America*, Vol. 61, No. 11, Nov. 1971, p. 1565.

[8] Cool, T. A., "Power and Gain Characteristics of High Speed Flow Lasers," *Journal of Applied Physics*, Vol. 40, No. 9, Aug. 1969, pp. 3563–3573.

[9] Laderman, A. J. and Byron, S. R., "Temperature Rise and Radial Profiles in CO_2 Lasers," *Journal of Applied Physics*, Vol. 42, No. 8, July 1971, pp. 3138–3144.

[10] Gerry, E. T., "Gas Dynamic CO_2 Lasers," *Bulletin of the American Physical Society*, Vol. 15, April 1970, p. 563.

[11] Meinzer, R. A., "Experimental Gas Dynamic Laser Studies," *AIAA Journal*, Vol. 10, No. 4, April 1972, pp. 388–393.

[12] Tsien, H. S. and Beilock, M., "Heat Source in a Uniform Flow," *Journal of the Aeronautical Sciences*, Vol. 16, No. 12, Dec. 1949, p. 756.

[13] Fuhs, A. E., Biblarz, O., Cawthra, J. K., and Campbell, J. L., "Experimental Verification of Density Inhomogeneity Due to Lasing in a Gas Dynamic Laser," *Applied Physics Letters*, Vol. 24, No. 3, Feb. 1974, p. 132.

[14] Fuhs, A. E., "Quasi Area for Heat Addition in Transonic and Supersonic Flight Regimes," TR-72-10, 1972, Air Force Aero Propulsion Laboratory, Wright-Patterson Air Force Base, Ohio.

[15] Fuhs, A. E., "Density Inhomogeneity in a Laser Cavity Due to Energy Release," *AIAA Journal*, Vol. 11, No. 3, March 1973, pp. 374–375.

[16] Hoffman, A. L. and Vlases, G. C., "A Simplified Model for Predicting Gain, Saturation, and Pulse Length for Gas Dynamic Lasers," *IEEE Transactions on Quantum Electronics*, Vol. QE-8, No. 2, Feb. 1972, pp. 46–53.

[17] Read, A. W., "Vibration Relaxation in Gases," *Progress in Reaction Kinetics*, Vol. 3, Pergamon Press, New York, 1965, pp. 203–235.

[18] Stollery, J. L. and Park, C., "Computer Solutions to the Problem of Vibrational Relaxation in Hypersonic Nozzle Flows," Rept. 115, Jan. 1963, Imperial College of Science and Technology, London, England.

[19] Taylor, R. L. and Bitterman, S., "Survey of Vibrational Relaxation Data for Processes Important in the CO_2-N_2 Laser System," *Reviews of Modern Physics*, Vol. 41, Jan. 1969, pp. 26–45.

[20] Vincenti, W. G. and Kruger, C. H., Jr., *Introduction to Physical Gas Dynamics*, Wiley, New York, 1965, pp. 198–206.
[21] Biblarz, O. and Fuhs, A. E., "Laser Internal Aerodynamics and Beam Quality," *Proceedings of the SPIE 17th Annual Technical Meeting, Developments in Laser Technology—II*, Aug. 1973, San Diego, Calif.
[22] Born, M. and Wolf, E., *Principles of Optics*, Pergamon Press, New York, 1965, pp. 109–132.
[23] Liepmann, H. W. and Roshko, A., *Elements of Gasdynamics*, Wiley, New York, 1957, pp. 153–157.
[24] Clark, P. O., "Design Considerations for High Power Laser Cavities," AIAA Paper 72-708, Boston, Mass., 1972.
[25] Tucker, J. W. and Dewitt, R. N., "Atmospheric Propagation with Thermal Blooming," NRL Rept. 7038, Dec. 1969, Naval Research Lab., Washington, D.C.
[26] Rosenstock, H. B. and Tucker, J. W., "An Upper Limit on the Thermal Defocusing of a Light Beam," NRL Memo. Rept. 2109, April 1970, Naval Research Lab., Washington, D.C.
[27] Hayes, J. N., "Thermal Blooming of Laser Beams in Gases," NRL Rept. 7213, Feb. 1971, Naval Research Lab., Washington, D.C.
[28] Hayes, J. N., "Thermal Blooming in Viscous and Thermally Conducting Fluids," NRL Rept. 7383, Aug. 1972, Naval Research Lab., Washington, D.C.
[29] Stone, J. M., *Radiation and Optics*, McGraw-Hill, New York, 1963, pp. 161–166, 188–209.
[30] Fuhs, A. E., "Wave Structure of Exhaust from Transonic Aircraft," *Journal of Aircraft*, Vol. 8, No. 4, April 1971, pp. 280–281.
[31] Pindzola, M., *Jet Simulation in Ground Test Facilities*, AGARDograph 79, Pergamon Press, New York, 1963.
[32] Ehlers, F. E. and Strand, T., "The Flow of a Supersonic Jet in a Supersonic Stream at Angle of Attack," *Journal of the Aerospace Sciences*, Vol. 25, Aug. 1958, pp. 497–506.
[33] Kawamura, R., "Reflection of Wave at an Interface of Supersonic Flows and Wave Patterns in a Supersonic Compound Jet," *Journal of the Physical Society of Japan*, Vol. 7, Sept.–Oct. 1952, p. 412.

AUGUST 1974 AIAA JOURNAL VOL. 12, NO. 8

Temperature Extrapolation Mechanism for Two-Dimensional Heat Flow

MURRAY IMBER*
Polytechnic Institute of New York, Brooklyn, N.Y.

Unlike the investigations reported in the literature which are restricted to the simpler one-dimensional heat flow situation, the current study presents an analytical solution to the inverse problem that is applicable to two-dimensional conduction systems for geometries of arbitrary shape; heretofore intractable even for the simplest geometries. From theoretical considerations, temperatures can be predicted at discrete locations throughout the conducting medium, when input data such as thermocouple responses are known at several interior locations. Particularly, the transient temperature behavior may be readily established on any of the bounding surfaces by suitable interior thermocouple positioning. To facilitate computation of the desired temperatures, the theory allows for a temporal power series approximation of the input or thermocouple data, as is the customary practice in an experimental program. From transform techniques, the resultant theoretical expression for the prediction temperature is generated, and it appears as a summation of repeated error integrals. The form of the solution is convenient for numerical evaluation. Several numerical examples are presented as an indication of the accuracy of the theoretical results.

Nomenclature

$A_{l,m}^{ij}, C_l^{ij}, b_n^{ij}, c_{l,n}^{ij}$ = general coefficients
a_l, a_l' = free parameters, $a_l^2 + (a_l')^2 = 1$
$f(t), g(t)$ = general functions of time
$f(\Delta), g(\delta)$ = defined by Eq. (5)
$i^n \operatorname{erfc} x$ = repeated error integral of variable x
l, m, n, q = summation indices
N = number of matched points per face
p = $(s/\alpha)^{1/2}$
s = Laplace transform variable
t = time variable
T = temperature
$\bar{T}$ = Laplace transform of temperature
x, y = space variables
α = thermal diffusivity
Δ = distance between thermocouples, $x_2 - x_1$
δ = distance between thermocouples, $y_2 - y_1$

Subscripts

1 = property along sampling path x_1 or y_1
2 = property along sampling path x_2 or y_2
i = property along sampling path x_i
j = property along sampling path y_j

Superscripts

i, j = property at position, $x = x_i$, $y = y_j$

Received July 17, 1973; revision received November 30, 1973. The author wishes to express his appreciation to R. T. Corry for his assistance in the numerical computations associated with the illustrative examples.
Index category: Heat Conduction.
* Professor, Mechanical Engineering Department.

Introduction

FOR one-dimensional conduction systems, an analytical solution to the linear inverse problem is presented in Refs. 1 and 2. In the main, the temperature extrapolation procedure owes its success to the following features: first, the method does not rely upon numerical evaluation of complex integrals that ensue as a consequence of the application of transform techniques. Second, successive differentiation of interior temperature or heat flux data is not required; consequently the degradation associated with the values of the higher order time derivatives is eliminated. Last, internal temperature responses at two positions within the solid forms the basis for temperature extrapolation rather than heat flux and temperature data at one position. In any experimental program, a determination of the interior heat flux may prove to be impossible, whereas the thermocouple responses are readily available.

In Ref. 1, the literature pertaining to the one-dimensional inverse problem is reviewed in detail; however, a survey of the